

# Introduction to the Abrupt Wing Stall Program

Robert M. Hall\*

*NASA Langley Research Center, Hampton, Virginia 23681-2199*

and

Shawn H. Woodson†

*Naval Air Systems Command, Patuxent River, Maryland 20670-1906*

The Abrupt Wing Stall (AWS) Program has addressed the problem of uncommanded, transonic lateral motions, such as wing drop, with experimental, computational, and simulation tools. Background to the establishment of the AWS program is given as well as program objectives. To understand the fundamental flow mechanisms that caused the undesirable motions for a preproduction version of the F/A-18E, steady and unsteady flowfield details were gathered from dedicated transonic wind-tunnel testing and computational studies. The AWS program has also adapted a free-to-roll (FTR) wind-tunnel testing technique traditionally used for low-speed studies of lateral dynamic stability to the transonic flow regime. This FTR capability was demonstrated first in a proof-of-concept study and then applied to an assessment of four different aircraft configurations. Figures of merit for static testing and for FTR testing have been evaluated for two configurations that demonstrated wing-drop susceptibility during full-scale flight conditions (the preproduction F/A-18E and the AV-8B at the extremes of its flight envelope) and two configurations that do not exhibit wing drop (the F/A-18C and the F-16C). Design insights have been obtained from aerodynamic computational studies of the four aircraft configurations and from computations quantifying the impact of the various geometric wing differences between the F/A-18C and the F/A-18E wings. Finally, the AWS program provides guidance for assessing, in the simulator, the impact of experimentally determined lateral activity on flight characteristics before going to flight.

## Nomenclature

$C_L$	=	lift coefficient
$C_l$	=	rolling-moment coefficient
$C_{l,rms}$	=	rms of $C_l$
$C_P$	=	pressure coefficient
$c$	=	local wing chord
$F_Y$	=	lateral stick force
$M_\infty$	=	Mach number
$x$	=	distance from the leading edge
$\alpha$	=	angle of attack, deg
$\beta$	=	angle of sideslip, deg
$\theta$	=	model pitch angle, deg
$\phi$	=	model roll angle, deg

## Introduction

THE Abrupt Wing Stall (AWS) Program has been an applied aerodynamics effort addressing uncommanded lateral motions, a challenge that has plagued a significant number of aircraft over at least the last 50 years. Although the impetus of this program was the wing drop encountered during the engineering-and-manufacturing-development phase of the F/A-18E/F Program, that aircraft's issues were resolved before going to production. Subsequently, the AWS program was charged with developing methods and procedures to analyze and predict uncommanded motions for future aircraft. Because of limited resources, the focus of the AWS Program has been on abrupt wing stall occurring on moderately swept wings at transonic speeds.

## General Background

There are three typical types of uncommanded motions at transonic speeds, known as heavy wing, wing drop, and wing rock.<sup>1</sup> The sketches in Fig. 1 depict typical time histories of the bank angle and pilot's lateral stick force as well as notional drawings of separation activity over the wing. Heavy wing is usually the result of a shock-induced trailing-edge separation. This separation blankets the aft portion of the wing, results in a loss of lift in that region, and can degrade aileron effectiveness. If this happens asymmetrically between left and right wings, the aircraft will begin to slowly roll off as if it is out of trim. Wing drop is much more abrupt in nature. It usually involves leading-edge separation or a rapid expansion of the shock-induced separation occurring over the wing. In either event the wing separation expands rapidly over a small change in angle of attack, and significant flow asymmetries can occur between the left and right wing panels. Very powerful rolling moments can be generated by the asymmetric wing flows, resulting in significant, uncommanded roll offs that can preclude precision tracking or maneuvering in the heart of the transonic envelope. Wing rock, the third class of motions, is closely related to wing drop, except that the motion is periodic and is usually limited in magnitude. It is usually marked by the presence of static lateral stability and the absence of roll damping.<sup>1</sup>

Understanding and calculating transonic stall progression for moderately swept wings can be very difficult.<sup>2</sup> The separation process, whether from shock/boundary-layer interactions, from leading edges, or from hinge lines, is viscous dominated and not amenable to simple linear methods. Furthermore, the flow is very three-dimensional in nature and includes shed vorticity, oblique shocks, and significant spanwise flow. The shock positions over the wings can also be unsteady in the stall angle-of-attack region, as will be illustrated by both experimental and computational studies of the preproduction F/A-18E.

Because of the complexity of the flow, it is very difficult to understand and resolve this problem during flight test. First of all, lack of understanding of critical flow phenomena leads to "cut-and-try" efforts, which result in expensive, time-consuming solutions that might not apply at other flight conditions. Flight-test vehicles are not usually instrumented to describe wing flowfields adequately. Furthermore, traditional fixes used to mitigate these types of abrupt stall

Presented as Paper 2003-0589 at the Aerospace Sciences Meeting, Reno, NV, 6 January 2003; received 7 July 2003; revision received 22 August 2003; accepted for publication 29 August 2003. This material is declared a work of the U.S. Government and is not subject to copyright protection in the United States. Copies of this paper may be made for personal or internal use, on condition that the copier pay the \$10.00 per-copy fee to the Copyright Clearance Center, Inc., 222 Rosewood Drive, Danvers, MA 01923; include the code 0021-8669/04 \$10.00 in correspondence with the CCC.

\*Senior Research Engineer. Associate Fellow AIAA.

†Aerospace Engineer. Associate Fellow AIAA.

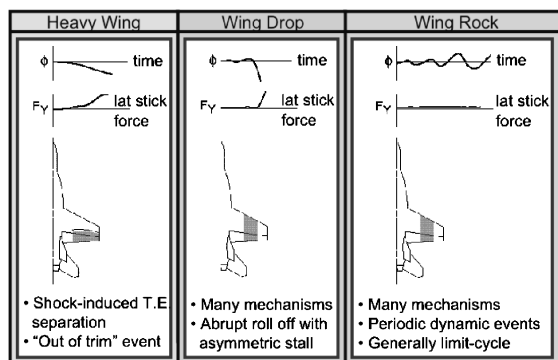


Fig. 1 Types of uncommanded, transonic lateral motions.



Fig. 2 Photo of the a) F/A-18E and b) F/A-18C in flight. Note snag on E leading edge.

issues in flight test, such as vortex generators, fences, or vortilons, can be detrimental to aircraft performance as well as signature. All of these factors point to the importance of being able to predict and mitigate uncommanded lateral motions before going to flight test.

#### F/A-18E/F Experience with Wing Drop

The immediate impetus for the AWS Program grew out of the F/A-18E/F development experience with wing drop. A photograph of the older F/A-18C and the more recent F/A-18E in flight is shown in Fig. 2. During 1996, test pilots in the F/A-18E/F program first identified an unacceptable wing drop as a potential maneuver problem at high subsonic and transonic speeds.<sup>3</sup> The first attempt to solve the wing drop was to modify the automatic leading-edge flap schedule by increasing the leading-edge flap deflections over an angle-of-attack range. The new flight-control laws were implemented and were found to significantly reduce the severity of the wing drop and its occurrence.<sup>3</sup> It did not, however, completely eliminate the problem. Furthermore, having residual wing drop was much more than a technical problem for the F/A-18E/F program. It also became a very undesirable political problem in late 1997. If a fix could not be found, it was very possible that the \$50 billion program<sup>4</sup> would have been canceled and that the U.S. Navy would have had difficulty in keeping an appropriate mix of aircraft on its carriers.

Unfortunately, conventional tools for configuration development and assessment—the wind tunnel and computational fluid dynamics (CFD)—were not reliable or timely to provide a solution to the problem. For example, when some promising modifications defined by wind-tunnel tests were implemented in flight tests only marginal improvement was realized in some cases. As a result of the com-

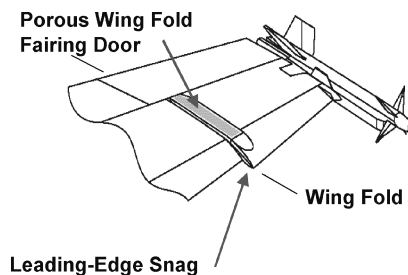


Fig. 3 Location of porous wing fold fairing door on F/A-18E wing.

plexity of the flow, progress in the application of Reynolds-averaged Navier–Stokes CFD tools to the problem was slow. Wind-tunnel oil flows and balance forces and moments were used to provide guidance to grid refinement and turbulence model selections.<sup>5</sup> On top of this initial delay, solution times were on the order of a week. The bottom line was that the wind-tunnel data were not considered reliable, nor the CFD results considered timely. Consequently, the burden to resolve the problem fell to the flight-test group, which evaluated over 100 configurations with over 10,000 evaluation maneuvers.<sup>6</sup>

As mentioned earlier, attempts to solve the wing-drop problem by increasing leading-edge flap deflections were partially successful. In fact, increased deflections were characterized as an 80% solution by the test pilots.<sup>3</sup> However, the Boeing Company and the U.S. Navy wanted more than an 80% solution, and so further steps were taken to improve the flying qualities of the airplane. The fix for the last 20% was the result of a Boeing test pilot, Ricardo Traven, suggesting that the wing fold fairing door be removed (see Fig. 3). Traven's background in aircraft icing issues led him to believe that the relatively large wing fold fairings on the F/A-18E wing could be adversely impacting the wing flow similar to an icing buildup, which is known to aggravate stall characteristics. He then suggested removing the wing fold fairing doors in an attempt to favorably impact the stall character of the airplane. Flight test verified that with the door off the airplane did not wing drop, although buffet was dramatically increased.<sup>3</sup>

When the news of the test flight without the wing fold fairing door was circulated in the F/A-18E community, personnel at NASA Langley suggested an obvious compromise between having no door (with no drop but high buffet) and a solid door (with wing drop but more acceptable buffet). The compromise, proposed by NASA, was to use a porous wing fold fairing door. The optimization process for the F/A-18E/F application was jump started because of previous work done on porosity at Langley.<sup>7,8</sup> Langley's experience and expertise were shared with Boeing and Naval Air Systems Command (NAVAIR), and Langley personnel were involved in determining the distribution of the porosity that was adopted for the production version of the aircraft and that solved the preproduction F/A-18E/F's wing-drop problem.

#### Impetus for AWS Program

During the investigation of the F/A-18E/F wing-drop problem, the U.S. Department of Defense commissioned a Blue Ribbon Panel to review the steps that Boeing and the Navy had taken to resolve the wing-drop problem. The Panel met informally in December of 1997 and then met formally during January and February of 1998 (Ref. 9). It concluded that 1) there was a lack of understanding of the abrupt stall process on the preproduction F/A-18E/F, 2) a broad-based research effort should be conducted to systematically study the wing-drop phenomena, 3) such a research effort should focus on developing figures of merit (FOMs) and design guidelines, and 4) the effort should identify and develop appropriate wind-tunnel test techniques and CFD codes that would be useful for predicting and solving this problem for future platforms.

To obtain approval for releasing this paper to the public, quantitative information has been removed from most vertical scales as directed by guidelines from the U.S. Department of Defense.

## AWS Program

The AWS Program was developed to meet the Blue Ribbon Panel recommendations. Consequently, its objectives included the development of technology for better understanding of the aerodynamic factors that cause abrupt wing stall, determining figures of merit for use in the interpretation of both wind-tunnel and CFD analysis, identifying design insights and guidelines, and developing test and analysis approaches for wind-tunnel, CFD, and piloted simulation work. Calibrations of the technical approaches were provided by experiments<sup>10–15</sup> and analyses<sup>16–21</sup> of the preproduction F/A-18E, the F/A-18C, the AV-8B, and the F-16C.

The initial emphasis of the AWS Program was on the F/A-18E in its preproduction form. This emphasis was necessary because a considerable amount of experimental, computational, and flight data appropriate for wing-drop analyses already existed for this aircraft. Although the literature suggested various possible FOMs for wing drop,<sup>22,23</sup> it was decided that the AWS Program would conduct in-depth correlations between ground-based and flight results to calibrate both FOMs and predictive methods.

The primary partners for the AWS Program have been NASA Langley and the U.S. Navy through the Office of Naval Research (ONR) and NAVAIR. NASA and ONR have contributed the bulk of the financial resources used during the program. The U.S. Air Force Research Laboratory at Dayton, Ohio, has also contributed funding to this program. Other governmental organizations that participated included NASA Ames Research Center, the F/A-18E/F Program Office (NAVAIR PMA 265), the AV-8B Program Office (NAVAIR PMA 257), and the Air Force F-16 Systems Program Office (ASC/YP). Industrial partners, who also contributed resources to this effort, have included Boeing and Lockheed-Martin. University involvement has encompassed the U.S. Air Force Academy, the Naval Postgraduate School, Notre Dame University, Virginia Polytechnic Institute and State University, the Naval Academy, and Princeton University.

## Highlights of the AWS Program

The technical approach to achieve the objectives of the AWS Program involved four phases, (see Fig. 4 and Table 1). The first phase involved taking advantage of the databases that already existed as a result of the F/A-18E/F wing-drop resolution effort. These legacy databases consisted of transonic wind-tunnel experiments with force-and-moment data and oil flows, Navier–Stokes computations, and flight-test data. The second phase was to develop databases that would fill in the flow understanding gaps from the existing F/A-18E databases. Specifically, the need was for more detailed wind-tunnel data and more computational efforts. To gain additional understanding of the stall process, a morphing study was conducted to explore the impact of the wing geometric differences between the preproduction F/A-18E and the F/A-18C. The third phase was to develop a dynamic wind-tunnel experimental method, assess FOMs for tunnel experiments as well as for CFD, and bring simulation tools to the problem. The fourth and last phase of the strategy was to assess the AWS-developed understanding, methods, and approaches on four different aircraft platforms—the preproduction F/A-18E, the AV-8B, the F/A-18C, and the F-16C. This last phase also defined a risk-reduction procedure to avoid uncommanded lateral motions for future aircraft.

### Legacy Data for F/A-18E/F and Other Aircraft

The first phase of the technical strategy involved mining the existing data sets that were developed by NAVAIR and Boeing during the development of the preproduction F/A-18E/F. From a wind-tunnel perspective, force and moment data, as well as oil-flow photographs existed, but no wing pressure data existed for the wing-drop conditions. Efforts by NAVAIR and Boeing to develop FOMs had not found a parameter that reliably predicted wing drop from the tunnel data for the preproduction F/A-18E for all flap combinations and Mach numbers. The NAVAIR/Boeing team did, however, recognize the importance of measuring the unsteadiness components of the

**Table 1 Four technical phases of AWS program**

Phase	Subelements
Analyze legacy data for F/A-18E and other A/C	Wind-tunnel data Force and moment Oil flows Legacy CFD and grids Flight data Historical review of transonic AWS experiences with other A/C
Flow understanding	Wind-tunnel diagnostics Pressures RMS values Pressure-sensitive paint Unsteady CFD Structured Unstructured Unsteady Impact of wing differences
Develop methods and approaches to predict abrupt stall	Transonic free-to-roll method FOMs for Wind tunnel CFD Simulation improvements and validation
Assess other configurations	One with activity (AV-8B) Two without activity (F/A-18C, F-16C) Calibrate FOMs for all configurations Correlate with flight Define recommended risk-reduction approach

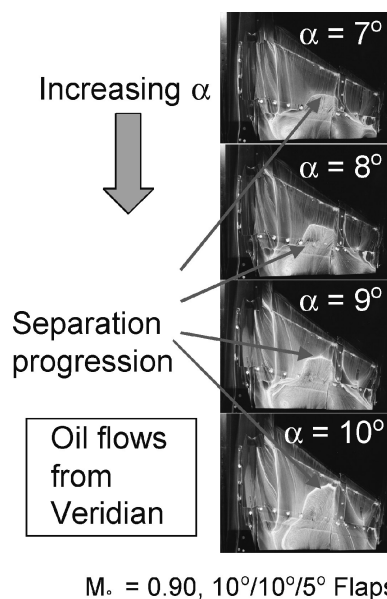


**Fig. 4 Progress of flow separation with angle of attack from legacy oil-flow images taken in the Veridian 8-ft transonic tunnel.**

balance forces and moments. This insight was very helpful to the AWS Program as it began its work.

Figure 4 highlights example oil flows taken at  $M_\infty = 0.90$  during testing of the F/A-18E in its preproduction configuration at the Veridian (formerly Calspan, Buffalo, New York) 8-ft transonic tunnel. (This preproduction configuration is the basis for much of the F/A-18E related research conducted in the AWS Program. The model had a solid wing fold fairing door—not a porous door as the production airplanes have. The flap setting of 10 deg/10 deg/5 deg summarizes, respectively, the leading-edge flap deflections, the trailing-edge flap deflections, and aileron bias.) As seen in the sequence of oil images, the flow is already separated at the trailing edge for an angle of attack  $\alpha$  equal to 7 deg. As the angle of attack is increased, the midwing stalled region progresses forward to a region just inboard of the leading-edge snag. Note the abrupt movement

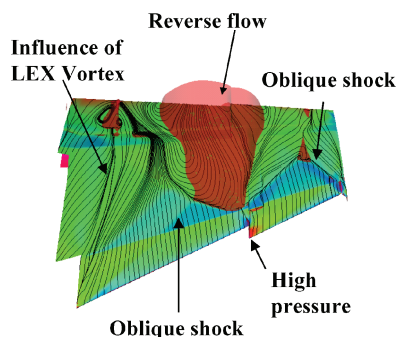


Fig. 5 Legacy CFD solution showing regions of separation for pre-production F/A-18E wing at wing-drop conditions:  $M_\infty = 0.90$  and  $\alpha = 9$  deg.

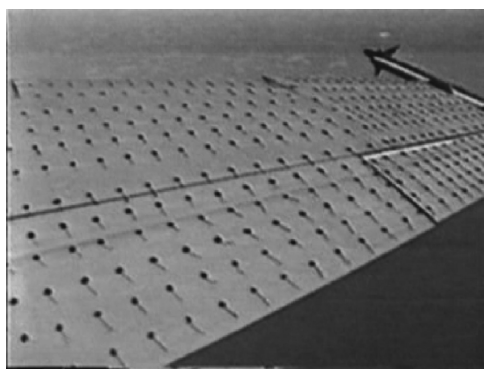


Fig. 6 Legacy F/A-18E flight video records with tufts illustrated regions of separation for F/A-18E wing in the wing-drop region.

of the stalled region toward the leading edge as the angle of attack increases from 9 to 10 deg.

Legacy CFD solutions were also a source of insight that was immediately useful to the AWS Program. An example of such a solution is shown in the Fig. 5. Even late in the development program, the main suspect for the abrupt stall properties of the F/A-18E was the pronounced “bump” associated with the thick wing fold fairing on the F/A-18E wing. However, the CFD solutions began to build the case that the leading-edge snag was dominating the separation process for the F/A-18E. As seen in Fig. 5, the separation pattern at  $\alpha = 9$  deg clearly shows a zone of separation approaching the leading-edge flap hingeline. Further AWS computations have found a connection between the snag and the unsteadiness in the position of the shock as wing stall occurs.<sup>17</sup>

As already mentioned, the existence of F/A-18E/F flight data and associated information was a tremendous asset to the AWS Program. In addition to having flight records that documented wing-drop conditions, limited visual records were also available. Some of these video records illustrated the progression of wing separation when the wing was tufted (see Fig. 6 for a typical tufted configuration). Also available were clips from chase-plane video when the F/A-18E exhibited naturally occurring flow visualization caused by condensation (see Fig. 7). These condensation video records illustrated that even at angles of attack below those for wing drop the flow pattern in flight was unsteady in nature. This unsteadiness was manifested by changes in the condensation pattern that appeared and disappeared as a function of time. These time-dependent changes, which appear as gaps in the condensation pattern, were attributed to unsteady separation. Still photographs of this video are shown in Fig. 7, which shows typical differences with time in the condensation pattern over the left wing panel.

As part of its data mining process, the AWS Program also sponsored a historical review of uncommanded lateral motions that had been experienced in past aircraft programs. The results of this study showed that many aircraft have had uncommanded lateral motions in the transonic speed range—heavy wing, wing drop, or wing rock, as is summarized in Fig. 8 (Ref. 1). In fact, the first example given is for



a) Note gap in condensation on left wing



b) Fuller condensation pattern moment later

Fig. 7 Naturally occurring condensation over the F/A-18E wing was unsteady near wing-drop angles of attack.

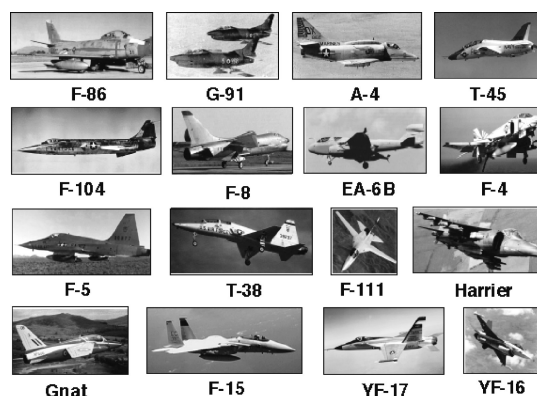


Fig. 8 Examples of high-performance aircraft that have had to deal with uncommanded lateral motions (see Ref. 1).

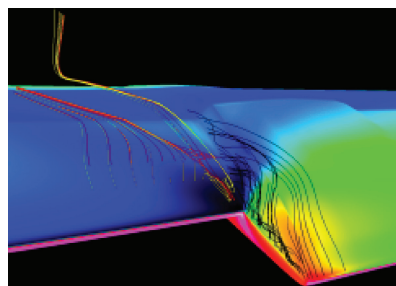
the F-86, the premier fighter of the Korean War era. It experienced wing drop, and that problem was mitigated with the addition of wing vortex generators. With many aircraft after the F-86 also having experienced uncommanded lateral motions at transonic speeds, it is clear that the preproduction F/A-18E/F experience was not an isolated case.

#### AWS Efforts Focused on Flow Understanding

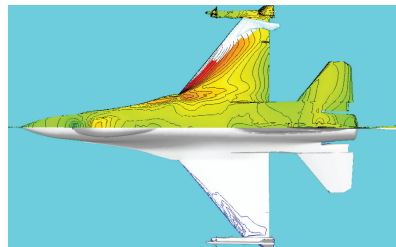
Although the legacy data were a rich source of information, the AWS Program needed more fundamental and detailed information in order to better understand the abrupt wing stall process. To address this requirement, a new highly instrumented wing was built for the 0.08-scale F/A-18E model previously used by Boeing and NAVAIR during the aircraft development program. The instrumentation added to this new wing included static pressures, unsteady pressure transducers, and wing-root bending gauges for each wing panel.<sup>10</sup> The experimental testing of the preproduction F/A-18E model emphasized the need to test with a sufficient number of flap settings to permit interpolation of data through the abrupt wing stall region.

Similarly, CFD efforts were expanded, and new computational codes were brought online to address the needs 1) to obtain more detailed comparisons to wind-tunnel data for the preproduction

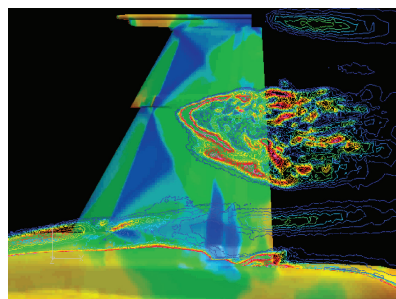




a) WIND code, F/A-18E snag flow



b) TetrUSS code, F-16C



c) COBALT code, unsteady flow over F/A-18E wing

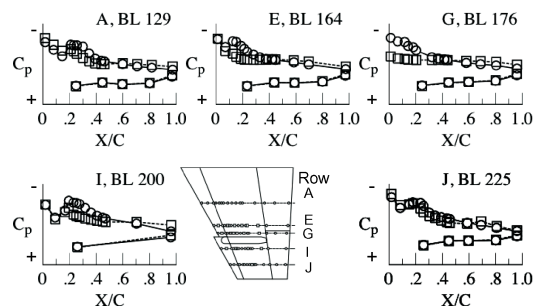
Fig. 9 Representative results of the CFD codes used.

F/A-18E, 2) to assess the impact of unsteadiness on the flow pattern over the F/A-18E wing, 3) to assess the impact of the wing design changes between the F/A-18C and the F/A-18E, and 4) to compute the flowfields over three other configurations explored by the AWS Program, the AV-8B, the F/A-18C, and the F-16C. The codes utilized, and representative results, are shown in Fig. 9. NAVAIR used the WIND code<sup>16,18</sup> that had been utilized by both Boeing and NAVAIR to generate the legacy solutions. WIND is a structured code that can be run in either a Reynolds-averaged Navier–Stokes (RANS) mode or a detached-eddy simulation (DES) mode. For the AWS computations it was utilized in the RANS mode. NASA and NAVAIR personnel both worked with the TetrUSS code.<sup>19,20</sup> This is an unstructured code that provided the flexibility to look at different geometries with a minimum amount of time and effort to create a new grid. TetrUSS was run in a RANS mode. Finally, the Air Force Academy used the COBALT code.<sup>17</sup> It is also an unstructured code and was used for this study in both RANS and DES modes. Its key contribution, however, was that it was used to generate several pioneering unsteady solutions that contributed to the understanding of unsteady aerodynamic factors important to abrupt stall.

During AWS wind-tunnel testing of the 0.08-scale F/A-18E model in the Langley 16-Foot Transonic Tunnel (16-ft TT) (see Fig. 10), two levels of effort were undertaken to capture the aerodynamic unsteadiness the model exhibited as it went through the stall process. The first level of effort was simply to route the signals from the gauges, accelerometers, balance, and unsteady pressure transducers through rms instrumentation that calculated running values of rms for the respective signals. The calculated values of the rms data were then recorded by the time-filtered tunnel data-acquisition system. Consequently, levels of unsteadiness were measured in addition to time-averaged values without going to the sizeable effort of recording time histories. This option is generally provided by wind-



Fig. 10 0.08-scale F/A-18E model in the Langley 16-ft Transonic Tunnel.

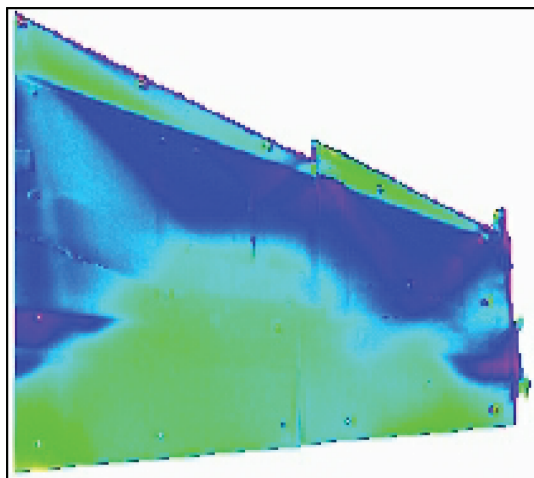
Fig. 11 Example steady pressures measured at  $M_\infty = 0.80$  for F/A-18E with flap settings of 10 deg/10 deg/5 deg;  $\circ$ ,  $\alpha = 8$  deg;  $\square$ ,  $\alpha = 9$  deg.

tunnel facilities at little or no charge and is an immense assistance for data analysis of abrupt stall tendencies. This rms signal does not, of course, contain any information as to the frequency or character of the time history. The second, and more resource intensive, level of unsteadiness measurement was to record the time histories of various parameters. Time histories were taken during the 0.08-scale F/A-18E model testing effort but required specialized instrumentation and a significant level of effort to reduce the data.<sup>11</sup>

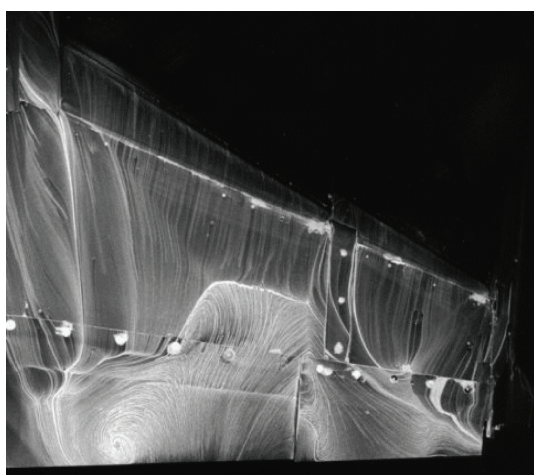
An example of the steady pressure distributions acquired is given in Fig. 11. Distributions are presented at angles of attack both below and above wing stall for a flap set of 10 deg/10 deg/5 deg. The pressure data are presented for various spanwise wing rows, or butt lines (see the middle sketch in the figure). The first pressure distribution, shown by the circular symbols, was taken at an angle of attack of 8.0 deg, before the stall occurred in the midwing region. The square symbols are for an angle of attack of 9.0 deg, which is after the stall for the wing panel at the midwing span locations. During the stall process, significant regions of low pressures—that is, coefficients toward the top of the vertical axis—collapse as the separation process progresses through the midwing region. Evidence of the stall process is apparent in rows A, E, G, and I, but is clearest in row G and is consistent with the legacy oil-flow images discussed earlier.

In addition to obtaining steady and unsteady pressure measurements, pressure-sensitive-paint (PSP) imaging was used to gather global information on the pressures influencing the wing drop. This technique, which offers the advantage of continuous pressure information across the wing (in contrast to the discrete pressure taps seen in Fig. 11), was highly successful in this transonic application. As seen in Fig. 12, the PSP pattern correlates well with comparable Veridian 8-ft transonic tunnel oil flows, despite the fact that the Veridian test used a different model wing than that tested at Langley. PSP images and their correlation with force-and-moment data are reported in more detail by McMillin et al.<sup>10</sup>

Both experimental work and computational work have been used to address the unsteady aspects of the flow over the F/A-18E wing. In Fig. 13a the image is an instant in time from time-accurate DES computations and depicts the vorticity being generated by the separated flow above the right wing panel of the F/A-18E at  $\alpha = 9$  deg and  $M_\infty = 0.90$  with 10-deg/10-deg/5-deg flaps. This image is from an animation, which shows a time-dependent pulsing of the shock forward and aft on the wing.



a) Langley PSP image



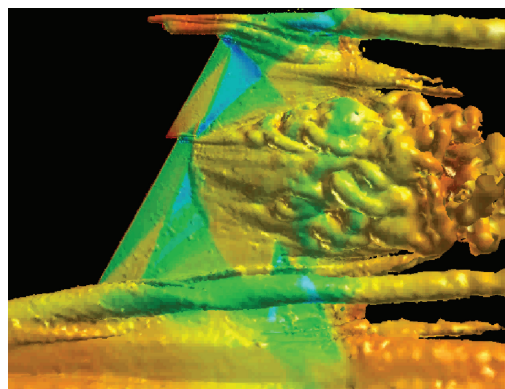
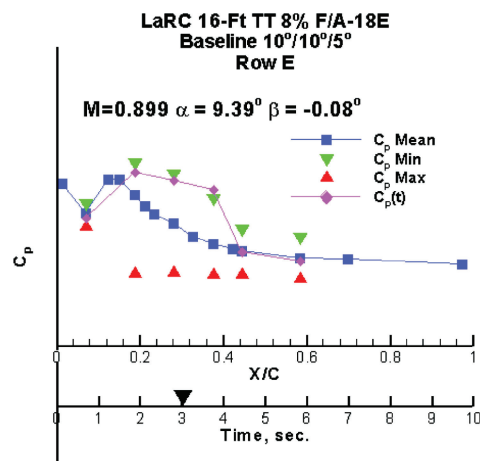
b) Veridian oil-flow image

**Fig. 12** Langley PSP image correlates well with Veridian oil flow. 0.08-scale F/A-18E model, Mach = 0.90;  $\alpha = 8$  deg; 10-deg/10-deg/5-deg flaps.

The graphic in Fig. 13b shows the experimentally measured wing pressure coefficients and their minimum and maximum values for six unsteady pressure transducers along row E, which is inboard of the snag (see Fig. 11). The minimum and maximum unsteady pressures at this flow condition, as illustrated by the orange and green symbols, depict the upper and lower pressure values that occur as the shock wave moves from a position close to 10% of local chord to a position close to 40% of chord. The pink symbols and line represent an instantaneous look at the unsteady pressures. For this case the shock is in the rearward location near 40%.

Both calculation and experiment are in qualitative agreement as to the magnitude of the pressure fluctuations and to the extent of shock movement.<sup>11,17</sup> The frequencies of the shock movement in both the experiment and computations are low enough to potentially result in a rigid-body response for the aircraft in flight. That is, the shock movement itself could trigger the wing-drop motion.

To gain further understanding of the abrupt stall process and to determine which wing geometric differences between the F/A-18C and F/A-18E were responsible for the sensitivity of the F/A-18E to wing drop, Green and Ott<sup>18</sup> computationally studied the impacts of leading-edge snag, the reduced leading-edge flap chord, the reduced leading-edge radius, the removal of the camber and twist, and the increased wing thickness. An example of the analyses by Green is presented in Fig. 14 for two modifications to the basic F/A-18C wing. Green also quantified the impact of each of these geometric differences on the angle of attack at which one would predict the onset of abrupt stall and loss of wing damping. In accomplishing his objectives, he also provided a potential figure of merit in the

a) Unsteady CFD,  $M_\infty = 0.90$ ,  $\alpha = 9.0$  deg

b) Wind-tunnel data

**Fig. 13** Unsteady DES computations and wind-tunnel measurements contribute to flow understanding.

form of the rate of change of sectional lift with angle of attack. Consequently, this important work provides a basis, for this class of wings, to conduct trade studies in the future between transonic maneuver capability and other mission requirements.

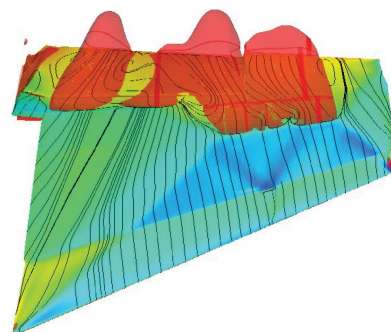
### Methods and Approaches

As shown in Fig. 4, the next technical approach after flow understanding was to develop methods and approaches for predicting abrupt wing stall and subsequent lateral activity. One of the key accomplishments was applying the free-to-roll wind-tunnel test technique<sup>13,14</sup> that had previously been used for subsonic flows<sup>24,25</sup> to the transonic speed regime. The development of figures of merit also fell within this task, as did simulation improvements.

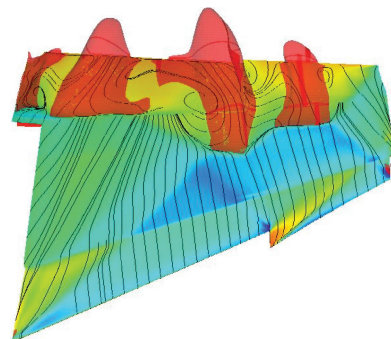
#### Free-to-Roll Test Technique

The application of the free-to-roll (FTR) technique to the transonic flow regime has been an important development for the AWS Program. This technique offers the promise of a robust diagnostic tool for determining the presence of uncommanded lateral motions. The uniqueness of this technique is that it allows the model to respond to static rolling moments (caused by asymmetries or sideslip) as well as dynamic rolling moments (damping in roll) with one degree of freedom about the body axis. A sketch illustrating the general relationships between  $\theta$ , strut angle, and  $\alpha$  and  $\beta$  as the model rolls about its body axis is shown in Fig. 15. The maximum value of  $\alpha$  occurs when the bank angle about the roll axis is zero. If the model were to roll to 90 deg of bank angle, then  $\alpha = 0$  deg and  $\beta = \theta$ .

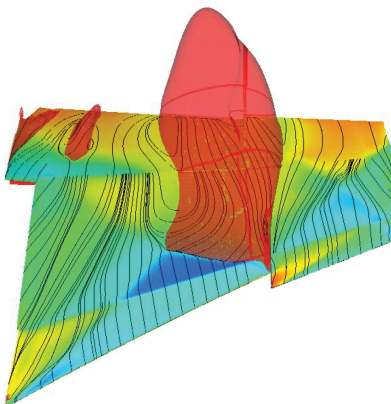
To assess the value of the FTR technique for transonic testing, a proof-of-concept experiment was conducted in the Langley 16-ft Transonic Dynamics Tunnel (TDT) in 2000. This test in the TDT utilized existing FTR hardware that had been previously used in the Langley 30- by 60-ft Wind Tunnel for low-speed tests. A lightweight 0.09-scale F/A-18E model was utilized for the experiment. The



a) Baseline F/A-18C



b) Baseline + snag



c) Baseline + snag + reduced leading-edge flap chord

Fig. 14 Flow solutions for basic and modified F/A-18C wing:  $M_\infty = 0.90$  and  $\alpha = 9$  deg.

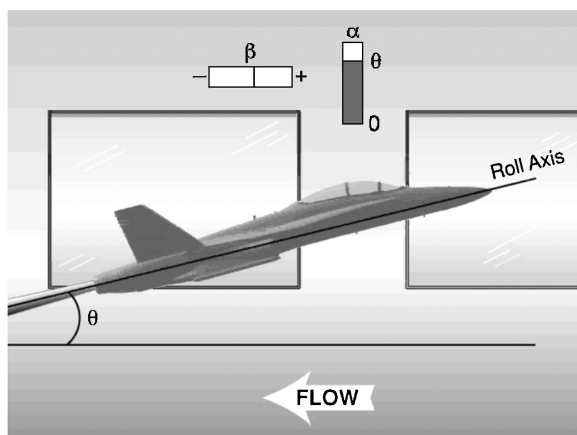


Fig. 15 General concept of free-to-roll testing, which allows model to rotate about body axis. Instantaneous values of  $\alpha$  and  $\beta$  will vary with bank angle of model.

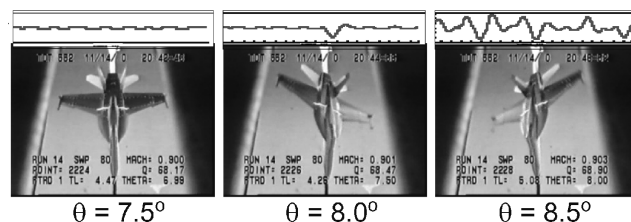


Fig. 16 Proof-of-concept test of FTR technique. Langley TDT tunnel. Representative bank angle vs time traces above images.

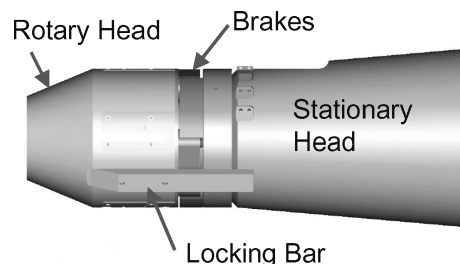


Fig. 17 Perspective of FTR apparatus used during 16-ft Transonic Tunnel test at NASA Langley. Stationary head mounts to tunnel support system.

FTR aspects of the test were remarkably successful. As illustrated in Fig. 16, different levels of FTR activity were detected that, for this configuration, related to lift-curve slope changes. The first photograph in the sequence shows the model at a wings-level condition for  $\theta = 7.5$  deg. At this attitude the wing had not yet stalled, and the model was relatively steady, reacting only mildly to tunnel turbulence. For the next higher value of  $\theta = 8.0$  deg, the model exhibited an occasional abrupt wing drop but was quiescent the majority of the time. When  $\theta = 8.5$  deg, an increase of only 0.5 deg, the model was in constant rolling motion with large-amplitude, limit-cycle wing-drop activity.

Based on the success of the proof-of-concept experiment in TDT, a completely new test apparatus (see Fig. 17) and technique were developed for the Langley 16-ft TT (Refs. 13 and 14). Because this new apparatus was designed accept a standard, metal, high-strength model, an objective of the new apparatus was to be able to integrate the FTR testing with the conventional stability and control testing in a seamless manner. Because the FTR rig also utilized the usual model balance and sting, there was no need to even dismount the model to put it on another apparatus in order to begin the FTR assessment. In practice, stability and control testing can proceed until static FOMs warn of potential problems, then the test engineer needs only to remove a locking bar, and the model can be assessed in a FTR mode.

#### Figures of Merit

Static figures of merit can be very important because they are intended to predict wing-drop behavior and, consequently, to enter into the decision of doing FTR testing or not. For example, some of the standard variables that have traditionally been proposed as FOMs are shown in Fig. 18. The first variable examined is the lift-curve behavior. Are there slope changes and how severe are they? The example illustrated shows a lift variation in which there is a very significant break in the lift-curve slope. Historically, such breaks have been regarded as possible indicators of major wing stall and potential asymmetries. The question faced by the designer is whether any of the lift beyond the kink in  $C_L$  is usable.<sup>22</sup> Another approach to potential figures of merit was taken by Bore,<sup>23</sup> where he reports that magnitude of rolling moment and the unsteadiness (rms) of rolling moment  $C_{l,rms}$  were utilized as FOMs in the design process for the British Harrier.

The importance of rms measurements, in general, and of  $C_{l,rms}$  was recognized by Boeing during the F/A-18E/F resolution effort and has been further investigated during the AWS Program. Use of



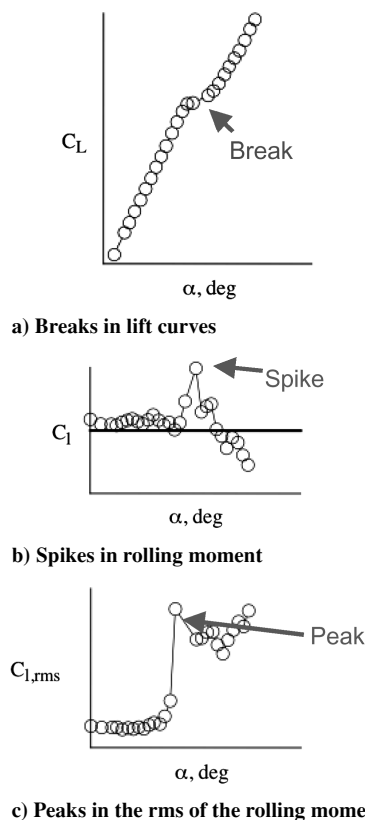


Fig. 18 Some traditional figures of merit that have been used to predict wing drop.

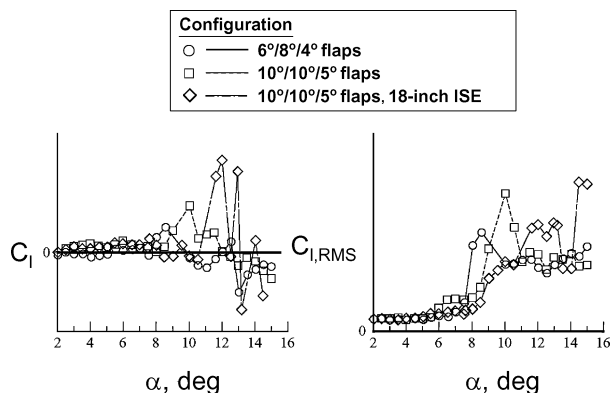


Fig. 19 Importance of rms measurements. More active nature of 6-deg/8-deg/4-deg flap set highlighted with  $C_{l,rms}$  but not with  $C_l$ .

$C_{l,rms}$  was found to be more helpful for studies with the F/A-18E than using trends in  $C_l$  asymmetries. In Fig. 19 a quick glance at the time-averaged values of  $C_l$  might suggest that the 6-deg/8-deg/4-deg flaps (circles) show relatively modest values of asymmetric  $C_l$ , and, therefore, this configuration might be a better choice than the 10-deg/10-deg/5-deg flaps (squares) or the third configuration (diamonds). This third configuration, which is the baseline configuration plus a snag extension that moves the snag 18 in. (0.46 m) inboard, also used flap deflections of 10 deg/10 deg/5 deg. However, based on flight experience, the 6-deg/8-deg/4-deg configuration exhibited more severe wing-drop behavior than either the 10-deg/10-deg/5-deg configuration (considered a better configuration) or the configuration with the 18-in. (0.46 m) inboard snag extension (considered the best configuration up and away but unacceptable because of powered approach issues). Two lessons can be learned from this example. First, time-averaged data, such as  $C_l$ , can exhibit a small mean value resulting from averaging unsteady measurements ranging from large positive to large negative values. Thus, it is important to consider the  $C_{l,rms}$  data, which clearly reflect the ordering

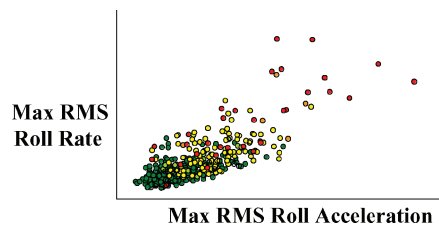


Fig. 20 Flight figure of merit identified, which looks at roll rate and roll acceleration. It generally separates green, yellow, and red events.

expected based on flight-test—activity first with the 6-deg/8-deg/4-deg flaps, activity second with the 10-deg/10-deg/5-deg flaps, and activity third with the 18-in. inboard snag extension.

The second lesson from Fig. 19 is the appearance of data gaps. Data gaps are a lack of experimental data at angles of attack where data should have been taken. They can be seen in Fig. 19 for 6-deg/8-deg/4-deg flaps at  $\alpha = 9.0$  and  $9.5$  deg, for 10-deg/10-deg/5-deg flaps at  $\alpha = 9.5$  deg and for the 10-deg/10-deg/5-deg flaps with the 18-in. inboard snag extension at  $\alpha = 11.0$  deg. For the 16-ft TT data these gaps occurred at angles of attack where model dynamics were so severe that data could not be safely taken and corresponded to conditions where the flow topologies over the wing were changing.

Lamar et al.<sup>12</sup> reports on the usefulness of the preceding FOMs, as well as wing root bending moments and other combination parameters. For CFD predictions of abrupt wing stall, the AWS Program found that either wing-root bending moment or half-plane bending moments were preferred figures of merit.<sup>16,19,21</sup>

#### Simulation Tools

Flying qualities and assessments of the relative severity of wing drop have also been a key area of research for the AWS Program. A breakthrough in this area occurred as the result of flight research and analysis conducted by the Transonic Flying Qualities Improvement Team, a Boeing/NAVAIR effort focused on exploring direct improvements to the F/A-18E/F. During the wing-drop resolution effort, analysis of the flight data was hampered by lack of an engineering metric. In other words, decisions were made on the basis of piloted assessments because it was not clear what combination of flight variables correlated with the pilot ratings. Fortunately, Roesch and Randall<sup>26</sup> brought order to this situation with their conception of a flight FOM that correlates well with the pilot ratings (see Fig. 20). Their flight FOM generally separated the trends of the green events (no lateral activity), yellow events (moderate activity), and red events (unacceptable lateral activity).

As mentioned, an effort was expended to determine how to improve the wind-tunnel data-acquisition process and its implementation into the simulator database. This study by Kokolios et al.<sup>27</sup> addressed the questions of how aerodynamic nonlinearities seen in wind-tunnel data should be implemented within the mathematical modeling package. Kokolios also identified the model structure needed within the simulation to properly represent the wing-drop event and validated these changes with piloted simulation results. This work has important implications for wind-tunnel testing, data entry into simulations, and modeling nonlinearities in the simulation. Furthermore, the simulation work of Kokolios found that the flight FOM of Roesch and Randall works well for fixed-base piloted simulation. Because of this research, it is now possible to quantify the impact of experimentally determined lateral activity on flying qualities in a piloted simulation before proceeding to flight.

#### Assessment of Other Configurations

The final phase of the technical approach of the AWS Program has been to assess the methods, approaches, and state of understanding with an examination of three additional configurations—the AV-8B, F/A-18C, and F-16C. These three configurations, along with the F/A-18E model, were tested on the FTR rig in the 16-ft TT at Langley. During these tests, conventional static data as well as FTR data were obtained. Detailed CFD calculations were





a) Preproduction F/A-18E



b) AV-8B at extremes of flight envelope

Fig. 21 Two aircraft susceptible to wing drop.



a) F/A-18C



b) F-16C

Fig. 22 Two aircraft not susceptible to wing drop.

also undertaken at tunnel-representative conditions for each of the four configurations. These configurations were carefully chosen for inclusion in the AWS Program efforts, being representative of two categories. The F/A-18E in its preproduction version without a porous door was susceptible to lateral activity, such as wing drop, as was the AV-8B in extreme regions of its flight envelope (see Fig. 21).

The other two configurations—the F/A-18C and the F-16C—are known not to exhibit wing-drop or wing-rock issues in flight and serve as excellent calibration configurations for the AWS-developed FOMs and test methods (see Fig. 22).

This assessment of four configurations has been absolutely critical to the success of the AWS Program. Without the broader look beyond the F/A-18E, it would have been easy to assume that the character of the lateral activity of the preproduction F/A-18E was general in nature, but, as will be seen,<sup>12,13,15</sup> there are differences between the preproduction F/A-18E and the AV-8B. Also, including two configurations that do not drop was important for proper validation of the static FOMs<sup>12</sup> and of the FTR technique itself.<sup>13</sup> Furthermore,



Fig. 23 0.15-scale AV-8B model mounted on the FTR rig in Langley 16-ft TT.

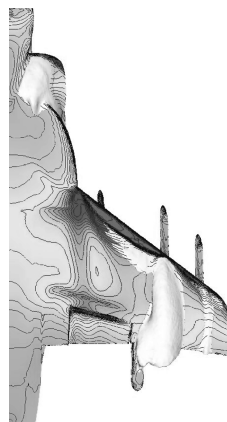
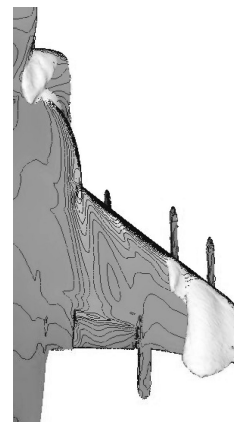
a)  $M_\infty = 0.75$ , TEF = 15 deg,  $\alpha = 8$  degb)  $M_\infty = 0.30$ , TEF = 25 deg,  $\alpha = 12.5$  deg

Fig. 24 Computational results for AV-8B showing Mach-number effects on separation after wing panel stall.

the CFD analyses conducted on these configurations have yielded important design insights.<sup>19,20</sup>

#### Experimental and Computational Analyses

The FTR testing of the AV-8B configuration (see Fig. 23), was extremely informative. First, the results changed the perceptions of the adequacy of static FOMs to predict wing drop and wing rock. For example, correlations between lift-curve breaks taken during concurrent static force testing and the onset of FTR lateral activity were good for the F/A-18E but were not as good for the AV-8B.<sup>12,13,15</sup> In fact, with the AV-8B there were examples during the FTR testing phase where it was clear in the video record that there was no lateral activity even though the model was obviously experiencing a wing stall process, as evidenced by longitudinal dynamics of the model on the sting. Although many candidate static FOMs were found to be deficient based on the FTR evaluation, the agreement between FTR activity in the wind-tunnel and recorded flight activity was excellent.<sup>13</sup>

The computational work on the AV-8B<sup>20</sup> also resulted in some interesting observations. Because experiment and computations were conducted at Mach numbers as low as 0.3, it was the AWS Program's opportunity to contrast transonic and subsonic stall character. An example of differences caused by Mach number is illustrated in Fig. 24. Figure 24a is for the transonic case,  $M_\infty = 0.75$ , and shows a midwing separation character similar to the case for the transonic F/A-18E. Figure 24b is for the subsonic case,  $M_\infty = 0.30$ , and illustrates a broader separation on the outer wing.

The test and analysis of the F/A-18C (see Fig. 25) also yielded some important insights.<sup>12,13,15,20</sup> This aircraft does not exhibit uncommanded lateral activity while flying on automatic flap schedule and FTR testing correlated with flight experience. In the AWS Program, however, the model was arbitrarily tested off flap schedule to obtain more data for correlation between static FOMs and FTR

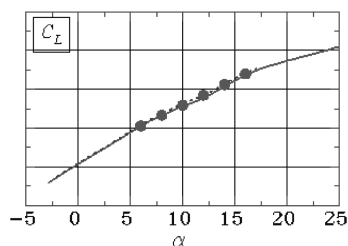


Fig. 25 0.06-scale F/A-18C model mounted on the FTR rig in Langley 16-ft TT.



Fig. 26 1/15-scale F-16C model mounted on the FTR rig in the Langley 16-ft TT.

Fig. 27 Computational results show smooth lift-curve properties of F-16C, where  $M_\infty = 0.80$ : —, VERIDIAN ( $RE/ft = 2.5$  million); - - -, 16-FT ( $RE/ft = 3.63$  million); and ●, CFD ( $RE/ft = 2.5$  million).



activity. These off-design conditions revealed that significant lateral activity was exhibited by the F/A-18C configuration with its flaps-off schedule. This result is an important reminder that predictions of uncommanded activity can be mitigated if the flap schedule can be modified to avoid the problem. This is not always successful, however, as evidenced by the F/A-18E experience.

The third additional configuration tested and computationally evaluated was the F-16C (see Figs. 26 and 27). Results of the studies were characterized by minimal FTR activity,<sup>13</sup> gradual onsets of wing stall,<sup>12</sup> and a smooth progression of sectional lift with angle of attack.<sup>19</sup> A comparison of computationally predicted and experimentally measured lift curve is shown in Fig. 27 for  $M_\infty = 0.80$ . The F-16C configuration was, generally, the most well behaved of the four configurations tested.

#### Recommended Screening Approach for Future Aircraft

It is now possible to outline a procedure to screen future configurations for abrupt stall issues before going to flight. The procedure is given in Fig. 28. It is envisioned to first conduct either a static wind-tunnel test or steady-state CFD computations for a candidate configuration. If static FOMs for either the wind tunnel or CFD flag a possible concern, then the next level of examination is needed. It is strongly urged, however, to proceed to the FTR level of testing if

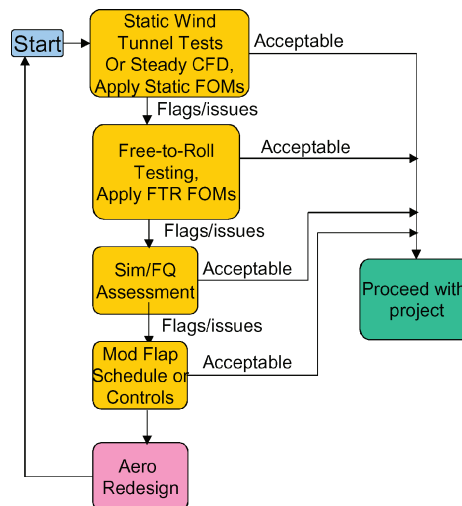


Fig. 28 Candidate AWS screening approach for future aircraft.

there is any possibility that the aircraft will have to operate at angles of attack approaching, or above, wing stall. As developed in papers by Lamar et al.,<sup>12</sup> Owens et al.,<sup>13</sup> and Capone et al.,<sup>15</sup> static FOMs are inadequate for any case except that for which the angles of attack needed for the mission requirements remain below those where wing panel stall would occur. This is considered an unlikely case for most modern combat vehicles, which routinely fly at attitudes above wing panel stall.

The next level in the procedure is FTR testing. (In the future this next level can include the option of time-accurate CFD calculations to simulate model dynamic response.) If the FTR tests indicate model lateral activity of concern, then several steps are available before having to consider a configuration design change. The first step is to conduct flight simulation including the measured rolling-moment asymmetries from the tunnel and representative levels of roll damping determined from computational or experimental methods. If the simulation shows that the aircraft cannot satisfactorily conduct its mission, then the second step is to ascertain if the flap schedule can be changed to avoid the problem or if the flight-control system can be enhanced to mitigate the problem. If those approaches fail, then a configuration change is a necessity. The key to the success of this screening process is using the FTR technique, which can correctly identify and characterize wing-drop tendencies.<sup>13</sup> Screening and risk reduction is also addressed by Cook et al.<sup>28</sup>

#### Summary

The AWS Program has addressed the problem of uncommanded lateral motions, such as wing drop, at transonic speeds. The problem has been attacked by coordinated computational and experimental studies of the abrupt separation process that governs the flow about the preproduction F/A-18E. This effort has involved transonic wind-tunnel testing, computational studies using three codes, simulation studies, and analyses of flight-test data.

An important contribution of the AWS Program is the application of the low-speed free-to-roll technique to the transonic flow regime. This new tool can be used for transonic tests with little extra tunnel occupancy time and provides a robust indicator of lateral activity. This dynamic, transonic test method has been correlated to known flight behavior and, in turn, has been used to evaluate traditional static figures of merit. The AWS Program has been able to evaluate four aircraft—two that were known to be susceptible to wing drop, the preproduction F/A-18E and the AV-8B at the extremes of its flight envelope, and two that do not exhibit wing drop, the F/A-18C and the F-16C. Utilizing four aircraft to evaluate the methods and figures of merit produced by the AWS Program has proven to be invaluable.

An additional area of contribution was in the area of CFD. The computational effort has addressed the following goals: 1) understanding the basic steady-state flowfield about the F/A-18E;

2) determining the role of unsteady flow over the F/A-18E; 3) analyzing the AV-8B, the F/A-18C, and the F-16C; and 4) evaluating the impact of the key wing geometry differences between the F/A-18C and the F/A-18E. Design insights have emerged from all of these efforts.<sup>16,18–21</sup>

Cutting-edge detached-eddy-simulation calculations and experimental measurements have also been performed that demonstrate the unsteady nature of the shock oscillations on the upper surface of the preproduction F/A-18E wing.<sup>11,17</sup> These calculations and experimental measurements are in good agreement. Significantly, both studies suggest that the unsteady shock motion over the wing occurs for frequencies that are low enough to result in rigid-body motion of the aircraft in flight. These results indicate that a potential trigger mechanism for the wing-drop event can be the unsteady shock movement itself.

Finally, significant simulation work has been done under the AWS program that can impact how future simulation mathematical models are constructed. It is essential, for example, for these simulation packages to be able to model representative inputs for asymmetries in rolling moment and for degradations in roll damping.<sup>27</sup> The finding of an appropriate flight figure of merit<sup>26</sup> has opened the door for better decision making in future flight-test programs<sup>28</sup> and for predicting wing drop in a simulator—an important tool for future programs.<sup>27</sup>

## References

- <sup>1</sup>Chambers, J., and Hall, R., "Historical Review of Uncommanded Lateral-Directional Motions at Transonic Conditions," *Journal of Aircraft*, Vol. 41, No. 3, 2004, pp. 436–447; also AIAA Paper 2003-0590, Jan. 2003.
- <sup>2</sup>Mabey, D., "Unsteady Aerodynamics: Retrospect and Prospect," *Aeronautical Journal of the Royal Aeronautical Society*, Vol. 103, No. 1019, Jan. 1999, pp. 1–18.
- <sup>3</sup>Traven, R., Hagan, J., and Niewoehner, R., "Solving Wingdrop on the F-18E/F Super Hornet, 1998 Report to the Aerospace Profession," *Proceedings of the 42nd Symposium Aerospace and High Technology Database*, Society of Experimental Test Pilots, Lancaster, CA, Sept. 1998, pp. 67–84.
- <sup>4</sup>Fulghum, D., "Navy Narrows F/A-18E/F "Wing Drop" Options," *Aerospace and High Technology Database*, Aviation Week and Space Technology 0005-2175, Vol. 148, No. 3, 19 Jan. 1998, p. 29.
- <sup>5</sup>Stokesberry, D., "CFD Modeling of the F/A-18E/F Abrupt Wing Stall—A Discussion of Lessons Learned," AIAA Paper 2001-2662, June 2001.
- <sup>6</sup>Hanley, R., Dunaway, D., and Lawson, K., "Operational Lessons from the F/A-18E/F Total Flight Control Integration Process," Paper 32, NATO, May 2000.
- <sup>7</sup>Bauer, S., and Hernandez, G., "Reduction of Cross-Flow Shock-Induced Separation with a Porous Cavity at Supersonic Speeds," AIAA Paper 88-2567, June 1988.
- <sup>8</sup>Wood, R. M., Banks, D. W., and Bauer, S. X. S., "Assessment of Passive Porosity with Free And Fixed Separation on a Tangent-Ogive Forebody," AIAA Paper 92-4494, Aug. 1992.
- <sup>9</sup>Harris, R., "March 4 Blue Ribbon Panel II Report," *Inside the Navy*, Vol. 11, No. 10, 16 March 1998, pp. 5, 6.
- <sup>10</sup>McMillin, S., Hall, R., and Lamar, J., "Transonic Experimental Observations of Abrupt Wing Stall on an F/A-18E Model," AIAA Paper 2003-0591, Jan. 2003.
- <sup>11</sup>Schuster, D., and Byrd, J., "Transonic Unsteady Aerodynamics of the F/A-18E at Conditions Promoting Abrupt Wing Stall," *Journal of Aircraft*, Vol. 41, No. 3, 2004, pp. 485–492; also AIAA Paper 2003-0593, Jan. 2003.
- <sup>12</sup>Lamar, J., Capone, F., and Hall, R., "AWS Figure of Merit (FOM) Developed Parameters from Static, Transonic Model Tests," AIAA Paper 2003-0745, Jan. 2003.
- <sup>13</sup>Owens, D., Capone, F., Hall, R., Brandon, J., Cunningham, K., and Chambers, J., "Free-To-Roll Analysis of Abrupt Wing Stall on Military Aircraft at Transonic Speeds," AIAA Paper 2003-0750, Jan. 2003.
- <sup>14</sup>Capone, F., Owens, D., and Hall, R., "Development of a Free-To-Roll Transonic Test Capability," *Journal of Aircraft*, Vol. 41, No. 3, 2004, pp. 456–463; also AIAA Paper 2003-0749, Jan. 2003.
- <sup>15</sup>Capone, F., Hall, R., Owens, D., Lamar, J., and McMillin, S., "Recommended Experimental Procedures for Evaluation of Abrupt Wing Stall Characteristics," *Journal of Aircraft*, Vol. 41, No. 3, 2004, pp. 448–455; also AIAA Paper 2003-0922, Jan. 2003.
- <sup>16</sup>Woodson, S., Green, B., Chung, J., Grove, D., Parikh, P., and Forsythe, J., "Understanding Abrupt Wing Stall with CFD," AIAA Paper 2003-0592, Jan. 2003.
- <sup>17</sup>Forsythe, J., and Woodson, S., "Unsteady CFD Calculations of Abrupt Wing Stall Using Detached-Eddy Simulation," AIAA Paper 2003-0594, Jan. 2003.
- <sup>18</sup>Green, B., and Ott, J., "F/A-18C to E Wing Morphing Study for the Abrupt Wing Stall Program," AIAA Paper 2003-0925, Jan. 2003.
- <sup>19</sup>Parikh, P., and Chung, J., "A Computational Study of the Abrupt Wing Stall (AWS) Characteristics for Various Fighter Jets: Part I, F/A-18E & F-16C," AIAA Paper 2003-0746, Jan. 2003.
- <sup>20</sup>Chung, J., and Parikh, P., "A Computational Study of the Abrupt Wing Stall (AWS) Characteristics for Various Fighter Jets: Part II, AV-8B and F/A-18C," AIAA Paper 2003-0747, Jan. 2003.
- <sup>21</sup>Woodson, S., Green, B., Chung, J., Grove, D., Parikh, P., and Forsythe, J., "Recommendations for CFD Procedures for Predicting Abrupt Wing Stall," AIAA Paper 2003-0923, Jan. 2003.
- <sup>22</sup>Ross, A., "Flying Aeroplanes in Buffet," *Aeronautical Journal*, Database Name Aerospace and High Technology Database, Vol. 81, Oct. 1977, pp. 427–436.
- <sup>23</sup>Bore, C., "Post-Stall Aerodynamics of the Harrier GR1," AGARD, CP-102, *Fluid Dynamics of Aircraft Stalling*.
- <sup>24</sup>Nguyen, L., Yip, L., and Chambers, J., "Self-Induced Wing Rock of Slender Delta Wings," AIAA Paper 81-1883, 1981.
- <sup>25</sup>Grafton, S., and Libbey, C., "Dynamic Stability Derivatives of a Twin-Jet Fighter Model for Angles of Attack from –10 deg to 110 deg," NASA TN-D-6091, Jan. 1971.
- <sup>26</sup>Roesch, M., and Randall, B., "Flight Test Assessment of Lateral Activity," AIAA Paper 2003-0748, Jan. 2003.
- <sup>27</sup>Kokolios, A., Cook, S., and Niewoehner, R., "Use of Piloted Simulation for Evaluation of Abrupt Wing Stall Characteristics," AIAA Paper 2003-0924, Jan. 2003.
- <sup>28</sup>Cook, S., Chambers, J., Kokolios, A., Niewoehner, R., Owens, B., Page, A., and Roesch, M., "An Integrated Approach to Assessment of Transonic Abrupt Wing Stall for Advanced Aircraft," AIAA Paper 2003-0926, Jan. 2003.